In Vitro Cell.Dev.Biol.—Animal
DOI 10.1007/s11626-010-9302-6

# The effects of space flight and microgravity on the growth and differentiation of PICM-19 pig liver stem cells

**Neil C. Talbot · Thomas J. Caperna · LeAnn Blomberg · Paul G. Graninger · Louis S. Stodieck**

Received: 6 October 2009 / Accepted: 16 January 2010 / Editor: J. Denry Sato


**Abstract** The PICM-19 pig liver stem cell line was cultured in space for nearly 16 d on the STS-126 mission to assess the effects of spaceflight on the liver's parenchymal cells—PICM-19 cells to differentiate into either monolayers of fetal hepatocytes or 3-dimensional bile ductules (cholangiocytes). Semi-quantitative data included light microscopic assessments of final cell density, cell morphology, and response to glucagon stimulation and electron microscopic assessment of the cells' ultrastructural features and cell-to-cell connections and physical relationships. Quantitative assessments included assays of hepatocyte detoxification functions, i.e., inducible P450 activities and urea production and quantitation of the mRNA levels of several liver-related genes. Three post-passage age groups were included: 4-d-, 10-d-, and 14-d-old cultures. In comparing flight vs. ground-control cultures 17 h after the space shuttle's return to earth, no differences were found between the cultures with the exception being that some genes were differentially expressed. By light microscopy both young and older cultures, flight and ground, had grown and differentiated normally in the Opticell culture vessels. The PICM-19 cells had grown to approximately 75% confluency, had few signs of apoptosis or necrosis, and had either differentiated into monolayer patches of hepatocytes with biliary canaliculi visible between the cells or into 3-dimensional bile ductules with well-defined lumens. Ultrastructural features between flight and ground were similar with the PICM-19 cells displaying numerous mitochondria, Golgi apparatus, smooth and rough endoplasmic reticulum, vesicular bodies, and occasional lipid vacuoles. Cell-to-cell arrangements were typical in both flight and ground-control samples; biliary canaliculi were well-formed between the PICM-19 cells, and the cells were sandwiched between the STO feeder cells. PICM-19 cells displayed inducible P450 activities. They produced urea in a glutamine-free medium and produced more urea in response to ammonia. The experiment's aim to gather preliminary data on the PICM-19 cell line's suitability as an in vitro model for assessments of liver function in microgravity was demonstrated, and differences between flight and ground-control cultures were minor.

**Keywords** Cell line · Culture · Hepatocyte · Liver · Microgravity

## Introduction

For the past 50 yr it has been of interest to understand what changes in biological structure and function occur in cells when they are taken into space and exposed to microgravity (Clavin and Gazenko 1975; Clement 2005). Of particular interest has been what changes occur in a multi-cellular organism's cells that may lead to disequilibrium in homeostatic mechanisms at the level of the cell, the organ, organ systems, or the body as a whole. To this end, comprehensive physiological measurements have been taken of animals and humans while in space or in various other proxies of weightlessness (Clavin and Gazenko 1975;

N. C. Talbot (✉) · T. J. Caperna · L. Blomberg · P. G. Graninger
USDA, ARS, Animal and Natural Resources Institute,
Animal Biosciences and Biotechnology Laboratory,
Beltsville Agricultural Research Center,
Bldg. 200, Rm. 13, BARC-East,
Beltsville, MD 20705, USA
e-mail: neil.talbot@ars.usda.gov

L. S. Stodieck
BioServe Space Technologies, University of Colorado,
Boulder, CO 80309-0429, USA

Published online: 24 March 2010

Clement 2005). Special attention has been directed toward the study of the most obvious and detrimental physiological changes that occur in humans while in space, and most of these changes arise from the microgravity environment, e.g., loss of bone and muscle mass. However, other organs or tissues that suffer less profound changes in response to space flight have also been studied. Among these is the liver which has been found to function normally during space travel for the most part.

The liver performs many vital functions to maintain homeostasis in the body (Guyton and Hall 2006). The liver is the body's central organ of metabolism and acts by absorbing and processing nutrients in blood taken up from the digestive tract—metabolized substances are then stored and released by the liver as needed by the body. Various biotransformation functions that occur in the liver are vital for the removal of toxic substances from the body. However, these same biotransformation functions can also change benign molecules to toxic forms or can eliminate medicinal molecules from the body before they have had time to produce a therapeutic effect. Other important functions of the liver include protein metabolism, the storage of vitamins and minerals, the production of non-essential amino acid, serum proteins, clotting factors, lymph, bile, and various hormones important for digestion and tissue growth, and the elimination of dead red blood cells, bilirubin, and ammonia. Finally, as the largest internal organ of the body, a key physiological property of the liver is its capacity to act as a blood pool, i.e., infusing blood into the systemic blood supply to compensate for blood loss or by expanding its blood volume to accommodate sudden increases in the body's overall blood fluid (Guyton and Hall 2006).

Because of the liver's importance, the liver has been the focus of several animal and human studies in space. Space flight produced smaller organs overall in comparison to ground-controls in a study of neonatal rat development, but the liver-to-body weight ratio did not change significantly (Miyake et al. 2002). Denisova et al. (1988) showed that mineral and water content of the livers of rats remained unchanged after exposure to microgravity for 1 wk, whereas, in some other organs, changes were found. Rat liver DNA replication was unaffected by space flight (Komolova et al. 1987). Assay of insulin binding to rat liver cell membranes showed similar results between flight and ground-control rats (Macho et al. 1991a). Also, rats flown in space for 20 d apparently lost polydeoxyribonucleotides in their spleens and thymuses, but their livers did not (Misurova et al. 1981). However, some marked changes in the liver have been found. In a study of newts in space, some liver pathology was found in the flight newts, although whether this was directly related to weightlessness was not clear (Yamashita et al. 2001). Total cytochrome P450 content and activity were reduced in the livers of rats following 14 d of space flight (Merrill et al. 1987; Merrill et al. 1990; Rabot et al. 2000), and other studies in rats have shown perturbations in liver carbohydrate and lipid metabolism. For example, increased liver triglyceride content (Ahlers et al. 1981), changes in fatty acid constitution (Abraham et al. 1981), and lower liver cholesterol content (Merrill et al. 1987) were found. However, in another study in rats, 13 d of microgravity exposure did not result in changes in liver lipid content (Popova et al. 1999). Marked elevations of the glycogen content of flight rat livers have been repeatedly measured, as have reductions in liver macrophages numbers (Abraham et al. 1981; Merrill et al. 1987; Racine and Cormier 1992). Some rat liver enzymes, e.g., for amino acid, lipid, steroid, and carbohydrate metabolism, were increased after 1 or 2 wk of space flight (Abraham et al. 1981; Nemeth and Tigranian 1982; Abraham et al. 1983; Merrill et al. 1987; Macho et al. 1991b), although some of these changes were not consistent across separate studies, and they also may be related to stress responses (Nemeth et al. 1981; Macho et al. 1982) or other physiological changes resulting from the weightless condition such as changes in body fluid distribution or blood flow (Clavin and Gazenko 1975; Tietze and Putcha 1994; Clément 2005).

Cell culture studies of isolated cells or cell lines have been undertaken in space in the hope of generating useful in vitro models from which more, and more varied, cellular gene and protein expression responses to microgravity can be obtained (Unsworth and Lelkes 1998). Among the represented cell types, a few cell culture studies have examined isolated liver cells, hepatocytes, or hepatic cell lines. Most of these hepatocyte cell culture studies were conducted with simulated microgravity on earth. For example, in NASA's rotating cell culture system (RCCS), a microgravity simulating cell culture device, it was shown that primary cultures of isolated human hepatocytes or small clumps of hepatocytes would grow as spheroids or as long (1–3 cm) 3-dimensional pieces of tissue having in vivo-liver-like histological and ultrastructural features. These large in vitro-produced clumps of human hepatocyte outgrowths were maintained in the RCCS for as long as 60 d (Khaoustov et al. 1999). More recently, ground-based simulated microgravity genomic studies of frog liver cells (Ikuzawa and Asashima 2008) and of the HepG2 human liver cell line (Khaoustov et al. 2001; Clement et al. 2007) have been published. The results showed some differences in global gene expression between simulated microgravity conditions compared with the 1 g controls. One in vitro liver cell study has been conducted in space and was a joint effort between NASA and StelSys, LLC. The study involved the culture of human liver cells that were analyzed for their ability to metabolize introduced xenobiotic com-

pounds and for global gene expression via microarray techniques (NASA Fact Sheet, http://www.nasa.gov/mission_pages/station/science/experiments/StelSys.html). However, the results of the study have apparently not yet been unpublished.

The PICM-19 cell line was derived from pig embryonic stem cells, i.e., the primary culture of purified pig epiblast tissue (Talbot et al. 1993; Talbot et al. 1994a; Brooks and Gardner 1997). As a cell line, the PICM-19 cells are unique in their ability to differentiate into either fetal hepatocytes or cholangiocytes (bile duct cells), the two cell types that comprise the parenchyma of the developing liver (Talbot et al. 1994b; Talbot et al. 1996; Talbot and Caperna 1998). PICM-19 hepatocytes are cuboidal cells with centrally located nuclei joined by tight junctions and desmosomes that form canalicular structures between the cells, i.e., they have the morphology of fetal pig hepatocytes (Talbot et al. 1994b). PICM-19 cells also display functional characteristics of fetal and adult hepatocytes including the production of serum proteins, inducible P450 activities, phase II xenobiotic metabolism reactions, ammonia clearance and urea production, and they are reactive to inflammatory cytokines such as interleukin-6 and tumor necrosis factor-alpha (Talbot et al. 1996; manuscripts submitted and in preparation). PICM-19 differentiation into cholangiocytes is marked by the self-organization of the cells into functional 3-dimensional ductules (Talbot et al. 1994a; Talbot et al. 1996; Talbot et al. 2002). These in vitro-produced bile ductules closely resemble bile ductules that have been produced in vitro from the culture of both fetal and adult pig liver tissue (Talbot et al. 1994b; Talbot and Caperna 1998). The PICM-19 ductule structures were shown to strongly express gamma-glutamyltranspeptidase, an enzymatic marker of cholangiocytes (Tanaka 1974; Ishii et al. 1989), and they responded to treatment with physiological levels of secretin and glucagon by basolateral to apical transport of culture medium into the lumen of the ductules with in vivo-like kinetics (Talbot et al. 2002).

Given the cellular attributes listed above, the PICM-19 cell line can act as an in vitro model of the liver and may be particularly relevant for modeling liver growth and differentiation. Furthermore, PICM-19 cells may usefully model liver cell functions as outlined above. With this in mind, a study was undertaken in conjunction with NASA to gather preliminary data on the effects of microgravity on PICM-19 cell growth and differentiation as a model for the growth and differentiation response of the human liver. While maintenance of the human liver in space appears to be without problem, the capacity of a human's liver to normally regenerate and repair itself in space, e.g., in case of injury, is one possible concern that the PICM-19 model might address. It was also of interest to see if the culture of PICM-19 cells in a microgravity environment offered any advantages that might be applied to specific biotechnological uses, such as improving the growth and function of the cells for use as the biological component of an extracorporeal bioartificial liver device (Sussman and Kelly 1995; Strain and Neuberger 2002; Sen and Williams 2003) or for the harvesting of liver-specific products, such as blood clotting factors.

The present study describes the effects of spaceflight and microgravity on the cell structure and cell function of PICM-19 cells grown as adherent monolayer cultures in Opticell culture units. The preliminary data generated by the study showed no marked differences between flight and ground-control cultures in terms of cell differentiation, cell structure, or metabolic function, although some differences were found in gene expression. The findings indicate that liver regeneration and repair could be expected to be normal, i.e., as on earth, should astronauts suffer acute liver damage while in space.

## Materials and Methods

*Cell Culture and Reagents.* Fetal bovine serum (FBS) was purchased from Hyclone, Logan, UT. Cell culture reagents including Dulbecco's phosphate buffered saline (PBS) without $Ca^{++}$ and $Mg^{++}$, media, trypsin-EDTA (0.025% trypsin, 0.43 mM EDTA), antibiotics, non-essential amino acids, and L-glutamine were purchased from Invitrogen, Gaithersburg, MD. PICM-19 stock cells were grown in 25 $cm^2$ tissue-culture flasks (T25; Greiner, Frickenhausen, Germany) on STO feeder-layers in a 50:50 mixture of DMEM–low-glucose and Medium 199 supplemented with 10% FBS, 2-mercaptoethanol, and nucleosides (10% DMEM/199) as described in Talbot and Paape (1996). STO mouse fibroblast (CRL 1503, American Type Culture Collection, Rockville, MD; STO denotes SIMS mouse strain, Thioguanine resistance, Ouabain resistance) were grown in DMEM–high-glucose supplemented with 10% FBS (10% DMEM) as previously described (Talbot and Paape 1996). STO feeder-layers were prepared by exposing a suspension of STO cells to 8 krad of gamma radiation prior to plating so as to render the STO cells incapable of cell division. Cultures were routinely maintained at 37°C in a 5% $CO_2$ atmosphere.

PICM-19 cells at passage 76 (P76) and P77 were cultured in Opticell units according to the manufacturer's instructions (BioCrystal Ltd, Westerville, OH) and were cultured on only one of the two inner Opticell surfaces. The Opticell was charged with 2 ml of a 4-ml or 8-ml suspension of PICM-19 cells (and an unknown amount of "carry over" STO feeder cells) taken up by trypsin-EDTA treatment of a T25 flask culture to effect an approximate 1:1 or 1:2 split ratio (1:1 for "young" cultures and 1:2 for "old cultures"; see below). That is, for PICM-19 cell

attachment in the incubator, the Opticell unit was inclined slightly so that the PICM-19 cell suspension only extends approximately 2 cm across the Opticell's cell culture surface at one end of the unit (Fig. 1*B*). This resulted in only about 12 $cm^2$ being covered by the PICM-19 cells after their attachment. Twenty-four hours later, the Opticell was charged with 8 ml of a suspension of cryopreserved STO feeder cells at a concentration sufficient to produce a monolayer of approximately $6\times10^4$ cells/$cm^2$ across the remaining open area of the Opticell's culture surface. This also brought the total medium volume (10% DMEM/199) within the Opticell to 10 ml. Opticell cultures were routinely maintained at 37°C in a humidified 5% $CO_2$ atmosphere.

Three sets of PICM-19 Opticell cultures were prepared at three separate times so that the cultures would be at three post-passage time points for the experiment and also to anticipate possible launch delays. That is, because the differentiation of the PICM-19 cells requires 2–3 wk post-passage culture time (Talbot et al. 1994a, 1996), the cultures were prepared so as to be 4, 10, and 14-d-old at the time of the STS-126 space shuttle launch. This way, since the PICM-19 cells start dividing approximately 3 d after passage, the 4-d cultures would grow and differentiate almost entirely in the microgravity condition, whereas in the 14-d cultures, the majority of the PICM-19 cells would have stopped dividing and were differentiating before launch. In the end, and for the analysis of the results, 10-d and 14-d cultures were both included and were combined into one experimental group termed "old" cultures. The 4-d cultures comprised the other experimental group and were termed "young" cultures. Accounting for the nearly16 d in space aboard the shuttle, the PICM-19 old cultures were 26 d and 30 d old (old group) and 20 d old (young group) when they arrived at Edwards Air Force Base in California at the end of the STS-126 mission.

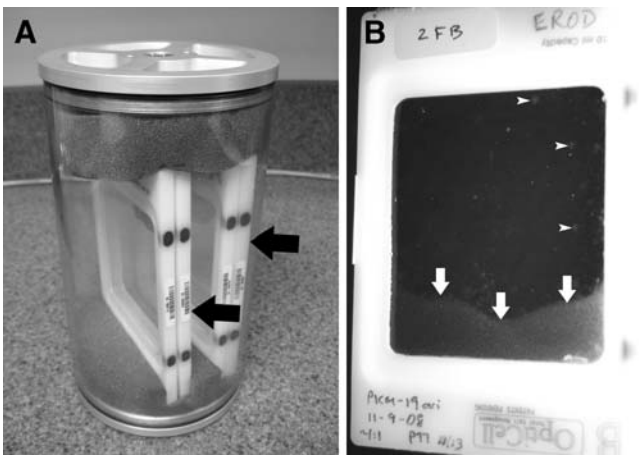


**Figure 1.** Composite figure showing a mock-up of a GAP unit with four Opticell culture units installed (*arrows*) in (*A*) and an actual Opticell culture unit photographed post-flight showing the PICM-19 cell monolayer at one end (*arrows*) and satellite-colonies (*arrowheads*) from pieces of the PICM-19 monolayer that broke off either in shipment to KSC or during lift-off, and then reattached to the Opticell culture surface at some point in time (*B*).

For spaceflight on the STS-126 experiment payload, the PICM-19 Opticell cultures were grouped in sets of four Opticell units per group activation pack (GAP; Fig. 1*A*) containment vessel—prepared with the assistance of BioServe Space Technologies, University of Colorado, Boulder, CO. A total of four GAPs were prepared for a total of 16 separate Opticell cultures. The groups were prepared by how old each culture was, i.e., days since being passaged or post-passage time. GAP #1G contained 4-d-old Opticell cultures for incubation on the ground (ground-control)—designated 1GA, 1GB, 2GA, and 2GB. GAP #1F contained 4-d-old cultures for launch and incubation in microgravity on the space shuttle (flight)—designated 1FA, 1FB, 2FA, and 2FB. GAP #2G contained two 14-d-old PICM-19 Opticell cultures (3GA and 3GB) and two 10-d-old cultures (4GA and 4GB) for use as ground-controls. GAP #2F contained flight cultures and included two 14-d-old cultures (3FA and 3FB) and two 10-d-old cultures (4FA and 4FB). Just prior to loading the Opticell cultures into the GAPs, the 10 ml of medium was evacuated from each Opticell unit and replaced with 15 ml of fresh 10% DMEM/199. This amount of medium was found to be sufficient, in preliminary ground-based tests, to maintain the Opticell PICM-19 cultures with no visible deleterious changes for up to 18 d. After the Opticell units were placed into the GAPs, the GAPs, with their lids ajar, were set inside a 37°C and humidified 5% $CO_2$ atmosphere incubator to equilibrate the atmosphere within the GAPs to 5% $CO_2$. The lids were secured on the GAPs, and each GAP was pressure-tested to insure and certify that they were air-tight by BioServe personnel. Thereafter, an attempt was made to keep the ambient conditions of light and temperature the same for all the GAPs during the time before launch, while on mission in space, and during the time after the GAPs returned to earth 16 d later. For example, STS-126 landed at Edwards Air Force Base, CA, and the GAPs were hand-carried in room temperature (rt) boxes during automobile and airplane travel back to Kennedy Space Center (KSC), a period of approximately 17 h. Therefore, the ground-controls at the KSC's Space Life Sciences Laboratory were removed from the incubator and kept at rt during the same time period.

For the actual STS-126 mission, flight GAPs were housed inside a flight thermal incubator, the Commercial Generic Bioprocessing Apparatus or CGBA (BioServe) and maintained throughout all phases of the mission, including launch, on orbit and landing, at 37°C±0.8°C. Ground-control GAPs were placed inside a standard $CO_2$ incubator and also maintained at 37°C. Launch of STS-126 occurred

approximately 30 h after the Opticell medium change, and the mission lasted 15 d, 20 h and 30 min.

Post-flight experimental assays were performed on ground and flight samples as described below. That portion of the Opticell polystyrene membrane to which the PICM-19 monolayer was attached was cut from the Opticell frame, and the membrane was cut into four equivalent pieces for assay or further processing, e.g., placed into 6-well plate wells with medium for metabolic assays or fixed in 2.5% glutaraldehyde for transmission electron microscopy examinations or the lysis of the cells in Trizol with immediate −80°C storage to prevent mRNA degradation (see below). The one-quarter membrane pieces were ~3 $cm^2$ in size.

*Post-Flight Subculture.* For post-flight subculture, PICM-19 cell monolayers from one Opticell membrane piece each for flight (2FA) and ground (2GA) were washed 2× with PBS and treated with trypsin-EDTA to release the cells from the Opticell membrane and produce a cell suspension. The cell suspensions of each were transferred into their own T25 flask containing a monolayer of irradiated STO fibroblasts at $6\times10^4$ cells/$cm^2$. Thereafter, the 2FA- and 2GA-derived cultures were passaged as previously described (Talbot et al. 1994a).

*Transmission Electron Microscopy.* Transmission electron microscopy (TEM) sample preparation and photomicroscopy were done with the assistance of JFE Enterprises, Brookeville, MD, as previously described (Talbot and Caperna 1998; Talbot et al. 2000). Ultrastructural analysis was performed on samples processed from Opticell cultures of two different ages. Including the nearly 16 d of culture time in space the cultures examined by TEM, flight and ground-control, were either 30 d old or post-passage (cultures 3FA and 3GA), or 20 d old or post-passage (cultures 2FA and 2GA).

*Assay of Cytochrome P450 1A1 and 3A Activities.* PICM-19 cell monolayers on Opticell membrane sections from flight (2FB and 4FA) and ground (2GB and 4GA) were assayed in triplicate by pre-incubating them with 5 μM 3-methylcholanthrene (3MC) in 1.5 ml of culture medium in 6-well tissue-culture plates (Corning-Costar, Corning, NY) for 24 h to induce CYPA1 [ethoxy resorfurin-*O*-deethylase (EROD)] activity. Cells were then exposed to Medium 199 medium with Hank's salts without L-glutamine and containing 8 μM 7-ethoxyresorufin (7-ERF), dicumerol (10 μM), and bovine serum albumin for 30 min as described by Donato and coworkers (1993). The medium was harvested, and the concentration of the reaction product, resorufin, was measured fluorometrically. Cytochrome P450 3A or benzyloxy-4-(trifluoromethyl) coumarin debenzylase (BFCD) activity was determined similarly following induction of the cells with 50 μM rifampicin (Rif) and subsequent incubation with phenol-red-free medium containing 7-benzyloxy-4-(trifluoromethyl) coumarin for 60 min. The reaction product, 7-hydroxy-4-(trifluoromethyl) coumarin (7-HFC), was quantified fluorometrically. All reagents were from Sigma-Aldrich (St. Louis, MO), and activity is presented as picomole product formed per 30 min/mg cell protein (EROD) or per 60 min/mg/protein (BFCD).

To determine the fluorescent products resorufin or 7HFC, experimental medium samples were incubated at 37°C with β-glucuronidase/arylsulphatase (15 Fishman/120 Roy units/ml, Roche Applied Sciences) in pH 4.5 acetate buffer for 2 h to release any fluorescent reaction product that had been conjugated via sulfation or glucurondation, viz. phase II conjugation reactions. Standard curves contained resorufin or 7-HFC and were treated identically to the experimental medium samples. Fluorescence was determined in an HTS 7000 microplate fluorescence spectrometer (Perkin Elmer, Waltham, MA); excitation/emission filter pairs were 530/590 nm and 410/510 nm for resorufin and 7-HFC, respectively. To determine relative conjugation activity, fluorescence was also determined directly without first incubating with β-glucuronidase/arylsulphatase. Since conjugated forms of resorufin and 7-HFC are non-fluorescent, the difference between the direct (without β-glucuronidase/arylsulphatase) and post-enzyme treatment (total) fluorescence measurements represents the amount of product which had been modified by conjugating enzymes.

*Urea Production Assay.* Opticell PICM-19 cultures (flight; 1FB, 4FB, and ground; 1GA, 4GB) were treated in situ by refeeding with glutamine-free Williams-E medium supplemented with 10% FBS, 1 mM ornithine, glucagon (100 ng/ml), 2-mercaptothanol (0.1 mM), HEPES (25 mM), and antibiotics for 48 h to stimulate urea production (Triebwasser and Freedland 1977; Metoki and Hommes 1984; Husson et al. 1987). One-quarter pieces of the PICM-19 monolayers were then exposed to the same base medium with or without the addition of 2 mM ammonium chloride in 6-well plates for 24 h. Medium was collected, centrifuged at 2,000×*g* to remove cellular debris, and frozen at −80°C prior to analysis. Urea concentration in medium was determined colorimetrically based on a diacetyl monoxime reaction assay described by the World Health Organization (Wybenga et al. 1971). Absorbance was determined at 540 nm, and a standard curve was prepared (NERL 2336; NERL Diagnostics, East Providence, RI). Values from base medium were subtracted from experimental samples.

*PICM-19 mRNA Isolation and RT-PCR Assay.* Total RNA was isolated from Trizol-cell lysates with the miRNeasy

Mini Kit (Qiagen, Valencia, CA) according to the manufacturer's instructions with the modification of using the Trizol-cell lysate rather than a Qiazol lysate for the initial cell lysis. An on-column digestion with DNase I (Qiagen) was performed to remove residual contaminating genomic DNA. Total RNA integrity and quantification were determined with the Agilent RNA 6000 Nano LabChip Kit on the Agilent 2100 Bioanalyzer (Agilent Technologies, Palo Alto, CA). Gene- and porcine-specific primers (Table 1) for select hepatocyte differentiation regulators or liver-specific transcripts, and β-actin were synthesized according to porcine-specific sequences obtained from GenBank (http://www.ncbi.nlm.nih.gov/entrez/query.fcgi) or the Gene Index Project at Harvard's Computational Biology and Functional Genomics Laboratory (http://compbio.dfci.harvard.edu/tgi/) porcine gene index databases. Two distinct β-actin primer sets were synthesized; one set that detected both mouse and pig β-actin and a second set that was pig-specific for real-time RT-PCR analysis (see Table 1).

Real-time RT-PCR was performed as previously described (Blomberg et al. 2005), except for the dilution of reverse transcription resultant cDNA product to 1.5 ng input RNA equivalents/μl) and the use of 5 μl of diluted cDNA product, in duplicate, in the real-time RT-PCR reaction. Thirty-three cycles of amplification were carried out in an ABI Prism™ 7000 Sequence Detection System (Applied BioSystems). The expression of the pig-specific β-actin was indistinct between flight and ground samples, so it was used as the endogenous control for the analysis ($C_T$s for ACTB shown in supplemental information). The RT-PCR products were analyzed, and the relative quantity (RQ) of the transcript was determined as previously described (Blomberg et al. 2005). The PICM-19 2FA sample was used as a calibrator to determine the RQ value for all genes examined; albumin (ALB), alpha-fetoprotein (AFP), transthyretin (TTR), heme oxygenase 1 (HMOX1), hepatocyte nuclear factor 1 alpha (HNF1A), hepatocyte nuclear factor 4 alpha (HNF4A), NF-kappaB (NFKB), manganese superoxide dismutase (SOD2), cytokeratin 8 (KRT8), cytokeratin 18 (KRT18), and met proto-oncogene (aka hepatocyte growth factor receptor; MET). The β-actin primer set common to both mouse and pig was included in each run as well for the amplification of β-actin in the STO cells and to provide further evidence of the specificity of the pig-specific primers.

**Table 1** Gene specific primers for different markers

| Gene | Primer | Database accession number |
|---|---|---|
| α-Fetoprotein | F: 5′-AGATGCCCATAAACCCTGGT-3′<br>R: 5′-CCAGTAGTCCAGAGAAATCTGCA-3′ | NM_214317 |
| Albumin | F: 5′-TGTTGCTGATGAGTCAGCTGA-3′<br>R: 5′-TGGAAGTCAGCGCATAAAGCA-3′ | NM_001005208 |
| Transthyretin | F: 5′-ATGGTCAAAGTCCTGGATGCT-3′<br>R: 5′-GATTTGGTGTCCAATTCCACT-3′ | NM_214212 |
| MnSOD | F: 5′-TAAAGTTCAACGGTGGAGGC-3′<br>R: 5′-AGCGGTCAACTTCTCCTTGA-3′ | X64057 |
| HNF1 alpha | F: 5′-CTGGCATCTTGCCTCTACTGGAAA-3′<br>R: 5′-CACGACTCAACCTGGCACCAA-3′ | NM_001032388 |
| HNF4 alpha | F: 5′-ACCAAGCGCTCTATGGTGTTTAAGG-3′<br>R: 5-′CACAGACACCCGGTTCATTTCTG-3′ | NM_001044571 |
| Met proto-oncogene (hepatocyte growth factor receptor) | R: 5′-GACCGGTTCATCAACTTCTTCGT-3′<br>F: 5′-TGCGTTTCCTTTAGCCTTCTCACT-3′ | NM_001038008 |
| NF-kappa-B | F: 5′-TAATGCTGGAATGAAGCACGGA-3′<br>R: 5′-TTCTGTGACTTTCCCAGAGAGA-3′ | NM_001048232 |
| Cytokeratin 8 | F: 5′-TGGGATGCAGAACATGAGTATCC-3′<br>R: 5′-TGGTAGGAGCTCAGGCTGTAGTT-3′ | NM_001159615 |
| Cytokeratin 18 | F: 5′-CAACGCCAGACCCAGGAGTA-3′<br>R: 5′-AAGATTGAAGTCCTCGCCATCTT-3′ | TC200462 |
| Heme oxygenase 1 | F: 5′-GTGCACGTCCAGGCTGAGAA-3′<br>R: 5′-ATGTGGTACAAGGACGCCATCA-3′ | NM_001004027 |
| B-actin, pig and mouse | F: 5′-TGTCCACCTTCCAGCAGATGT-3′<br>R: 5′-ATGCAACTAACAGTCCGCCTAGA-3′ | U07786 |
| B-actin, pig-specific | F: 5′-TCCTTCCTGGGCATGGAGTC-3′<br>R: 5′-GTGTTGGCGTAGAGGTCCTTC-3′ | U07786 |

## Results

*Microscopic Observations of PICM-19 Cells After Space Flight.* PICM-19 cells were flown in Opticell units without medium exchange for the duration of the flight. The PICM-19 cells grew and differentiated normally during their 16-d exposure to microgravity aboard the Space Shuttle Endeavor's isothermal containment module. That is, they proliferated to reach approximately 75% confluency and then stopped growing. This was evident in that both the young cultures and the old cultures were similar in appearance, but more importantly, in their degree of confluency. There were no apparent differences in morphology and differentiation status of the cells when comparing ground to flight cultures (Fig. 2). Both flight and ground-control cultures created monolayer patches of hepatocytes with biliary canalicular connections visible at their cell-to-cell junctions (Fig. 2*A*, *B*), and both flight and ground-control cultures had areas where the PICM-19 cells had self-organized into 3-dimensional bile ductules (Fig. 2*E*, *F*). That the cells were both equally functional, flight vs. ground-control, was first evident by their response to glucagon treatment. After a 30 min exposure to 0.1 μg/ml glucagon, the biliary canaliculi were inflated by transcellular fluid transport into the canalicular space (Fig. 2*C*, *D*).

*Subculture of PICM-19 Cells Following Exposure to Microgravity.* PICM-19 cells from one flight Opticell (group 2FA) and one ground-control Opticell (group 2GA) were passaged by trypsin-EDTA treatment to see if there were any obvious differences in growth efficiency or morphology with subsequent continuous culture under standard conditions, i.e., on STO feeder-layers in T25 flasks at 5% $CO_2$ and 37°C. The two PICM-19 cultures

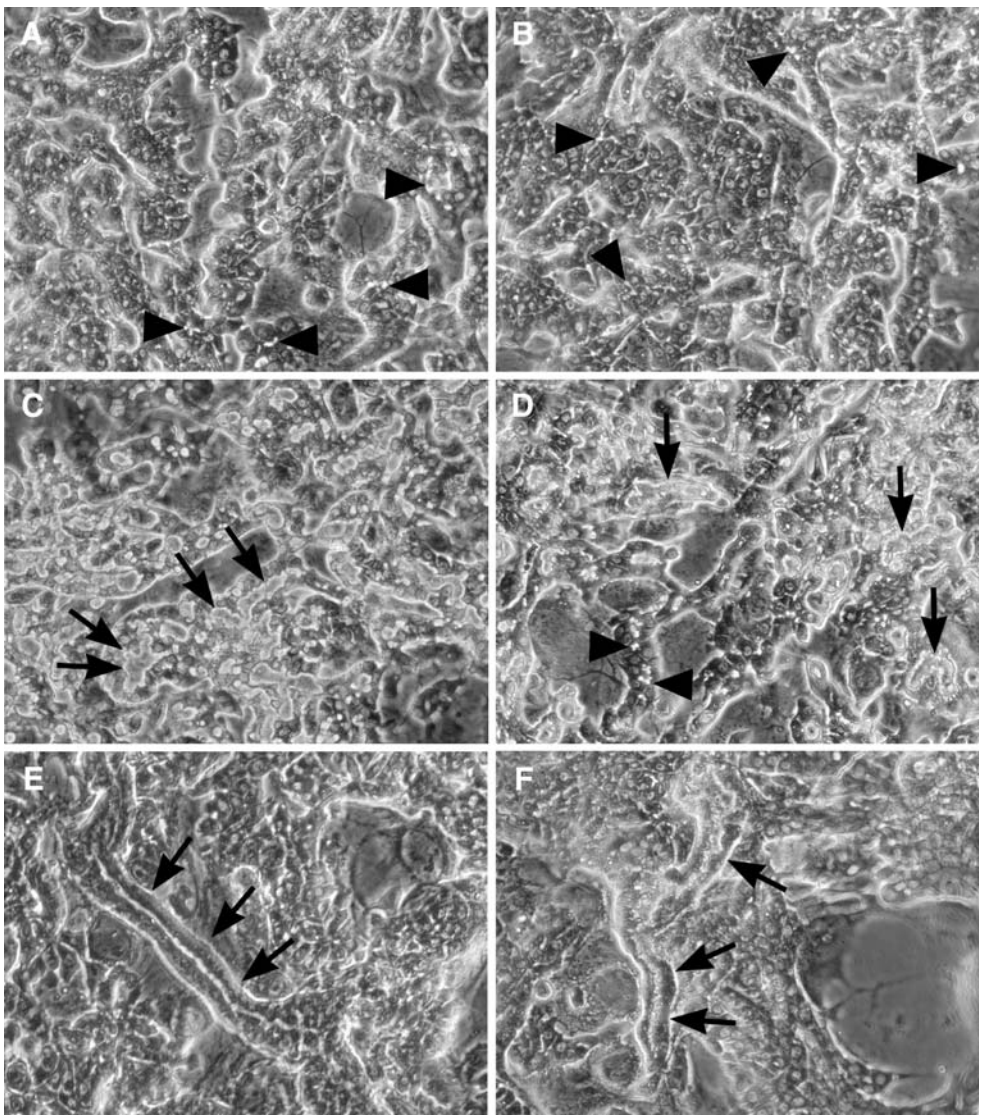


**Figure 2.** Phase-contrast micrographs of PICM-19 cell cultures after recovery from the Space Shuttle Endeavor's STS-126 mission. Panel *A* is Opticell 2FA (young flight culture) in comparison to panel *B* ground-control 2GA (young ground culture); *arrowheads* indicate examples of biliary canalicular structures normally found between differentiated hepatocytes. Panels *C* and *D* show the effects of exposing flight (1FB) and ground (1GA) PICM-19 cultures, respectively, to glucagon-containing (0.1 μg/ml) medium; note the gross expansion of the biliary canaliculi resulting from glucagon-stimulated transcellular fluid transport (*arrows*), although some biliary canaliculi, while distinct in appearance, remain less inflated (*arrowheads*). Panels *E* and *F* show 3-dimensional bile ductules (*arrows*) that formed from the self-organization of numerous PICM-19 cells during the course of the experiment in both flight (3FA; old culture) and ground-control (3GB; old culture) cultures. All micrographs were ×200 magnification.

were passaged 11 times over a period of 5 mo post-flight at the usual split ratio of 1:3 on STO feeder cells. No difference by microscopic assessments in plating and growth efficiency or in morphology and differentiation potential (both normal) were apparent between the two cultures over this time. Since there was no detectable difference in growth rate between the two cultures by visual inspection, comparative enumerative growth curves were not produced for the cell lines. The 2FA and 2GA passage 11 post-flight cultures were frozen in liquid nitrogen storage for possible future analysis.

*Transmission Electron Microscopy Analysis of PICM-19 Cells After Exposure to Microgravity.* The ultrastructure features of the flight and ground-control PICM-19 culture samples were similar to each other and also were similar to those of PICM-19 T-flask cultures previously reported (Talbot et al. 1996). Comparative analysis of flight and ground PICM-19 cultures showed that in both, the cells were closely associated with one another by extensive plasma membrane foldings that interdigitated along their lateral surfaces, and the cells were often found sandwiched between STO feeder cells (Fig. 3*A*). Biliary canaliculi were also frequently observed between two or more adjacent cells (Fig. 3*A*, *F*). Junctional apparati typical of polarized epithelial cells were found between adjacent PICM-19 cells at their lateral apical surfaces, i.e., facing the lumen of the biliary canalicular spaces (Fig. 3*C*). These tight-junction-like unions established the impermeable boundaries of the biliary canaliculi that existed between adjacent PICM-19

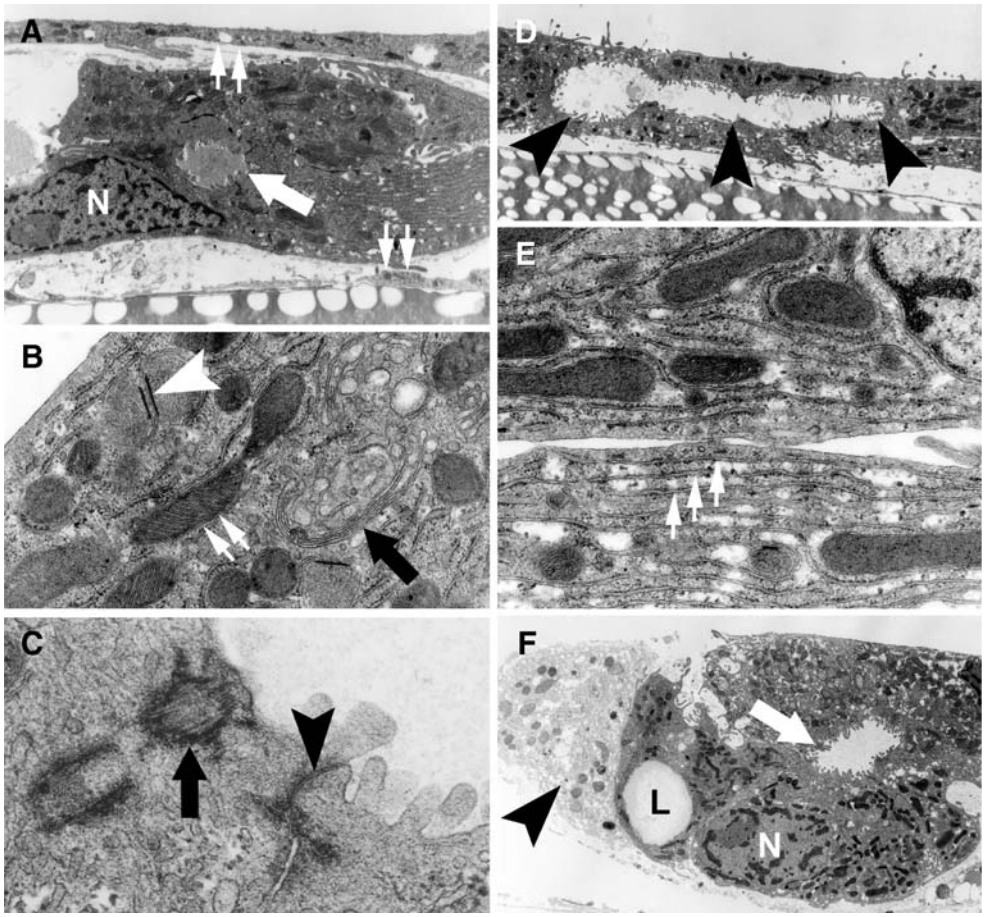


**Figure 3.** Transmission electron micrograph collage of flight and ground samples of PICM-19 cells grown in Opticell units. *A*, Flight sample showing biliary canliculi (*arrow*) formed by the apical membrane union of three PICM-19 cells. *Double arrows* indicate the STO feeder cells that arranged themselves above and below the PICM-19 cells. Opticell membrane support is fenestrated material at bottom of the panel (×18,900). *B*, Golgi complex (*black arrow*), mitochondrion (*double white arrows*) and peroxisome-like bodies (*white arrowhead*; ×75,000). *C*, Basal body of cilium (*arrow*) indicating its presence in the lumen of a bile ductule formed by the PICM-19 cells during flight. Note tight-junction-like union (*arrowhead*) between two PICM-19 cells at the apical surface, i.e., biliary canaliculus (×60,000). *D*, Bile ductule formed by several PICM-19 cells (*arrowheads*) in flight sample (×9,450). *E*, Rough endoplasmic reticulum surrounding mitochondria and showing typical stacked layers (*arrows*; ×48,000). *F*, Ground-control sample showing biliary canaliculi (*white arrow*) formed by the apical membrane union of 3 or 4 PICM-19 cells. Note lipid droplet in one of the cells (*L*) and the necrotic PICM-19 cell at *left* (*black arrowhead*; ×7,500). *N* nucleus.

cells as previously shown by ruthenium red staining (Talbot et al. 1996) and as shown here by glucagon-stimulated expansion of the canaliculi (Fig. 2*C*, *D*). The biliary canalicular surface had numerous microvilli that protruded into the canalicular space (Fig. 3*C*). The nuclei of the cells were generally oval and often had a single deep invagination (not shown). Rough endoplasmic reticulum was well represented in the cells and was often found in extensive stacks that surrounded some of the mitochondria of the cells (Fig. 3*E*). Smooth ER also appeared to be present in the cells, but it was difficult to discriminate from Golgi complexes with certainty since they were well-developed and numerous (Fig. 3*B*). Mitochondria were elongate (2–3 μm in length) in longitudinal section and oval (0.2–0.3 μm in diameter) in cross-section (Fig. 3*B*, *E*). Their lamellar cristae characteristically traversed the inner space of the mitochondrion. Membrane-bound bodies resembling peroxisomes were numerous, and some had electron-dense plate-like structures arranged parallel with their interior membrane (Fig. 3*B*). Relatively "empty" areas of cytoplasm with residual glycogen-like granules in them were frequently observed in the PICM-19 cells (Fig. 3*E*). Presumably, these were areas of glycogen storage where the glycogen was mostly lost as a result of inadequate glycogen rosette fixation. The PICM-19 cells also occasionally contained large lipid vacuoles (Fig. 3*F*), and secretory vesicles that were similar to or darker in electron density than that of the surrounding cytoplasm and, as is typical of the mucin-containing vesicles of gallbladder epithelium (Gilloteaux et al. 1997), they often contained an eccentrically located dense spherule (not shown). A cilium basal body was found in one of the many cells examined, and, therefore, cilium appeared to occur infrequently, indicating that at least some of the cells were probably monociliated with mechanosensory cilia (Fig. 3*C*)—typical of in vivo pig biliary canaliculi (Singh and Shahidi 1987). As previously observed in T-flask cultures of PICM-19 cells, a collagen fibril matrix was evident between the STO feeder cells and the PICM-19 cells, presumably having been produced by the STO fibroblasts (Fig. 3*A*).

*P450 Activity in PICM-19 Cells Exposed to Microgravity.* 3MC-induced cytochrome P450 1A1 activity (EROD activity) was measured in flight and ground-control PICM-19 culture samples by conversion of 7-ERF to the highly fluorescent product resorufin (Fig. 4). Measurement of direct (non-conjugated) resorufin in the medium was similar for flight and ground samples. However, when the activity of the old cells was compared with young cells, the old cells had secreted significantly ($P<0.05$) higher amounts of non-conjugated resorufin, indicative of lower overall phase II metabolic activity in the older cultures. Total EROD activity, as determined following treatment with β-glucuronidase/arylsulfatase, was higher as expected and indicated that a large percentage of the resorufin was further processed by phase II activities in the PICM-19 cells. Total EROD activity was similar for flight and ground samples and for young and old cultures, as well.

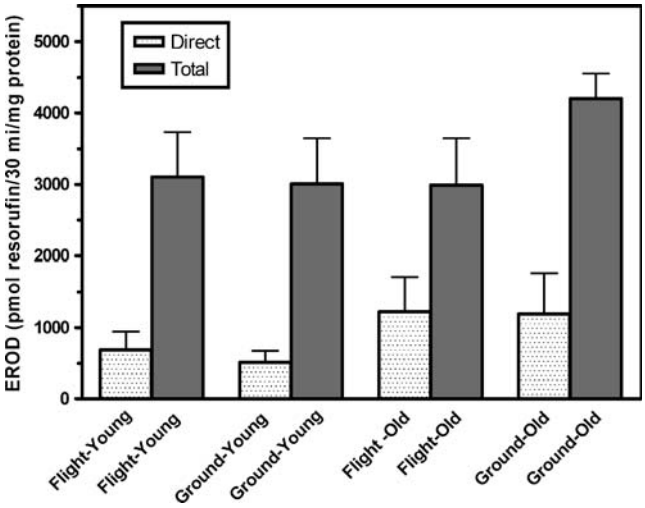


**Figure 4.** Induction of cytochrome P450 activity in 16-d flight and ground-control PICM-19 cultures by 3-methylcholanthrene (3MC). Culture samples ($n=3$) were exposed to 5 μM 3MC in complete medium for 24 h, after which the induction medium was replaced with specific enzyme substrate buffer for the detection of EROD activity as described in Materials and Methods. Young and old cultures designate 4-d-old and 10-d-old cultures, respectively, on the shuttle launch. Direct P450 activity is without treatment of samples with β-glucuronidase/arylsulfatase (see Materials and Methods). Data were analyzed by 2×2 ANOVA.

Inducible BFCD activity was also demonstrated in young flight and ground-control PICM-19 cultures (Fig. 5). In this instance, only young cultures were available for assay, and as observed with EROD activity, most of the coumarin-based metabolite of the BFCD assay was phase II-conjugated and required treatment with β-glucuronidase/arylsulfatase to be detected. There was no statistically significant difference between flight and ground-control PICM-19 cultures.

*Urea synthesis in PICM-19 Cells Exposed to Microgravity.* Both flight and ground-control PICM-19 cells produced urea and produced more urea after the addition of ammonia to the medium (Fig. 6). In terms of absolute amounts of urea produced, the young flight and ground PICM-19 cultures that were 20 d post-passage at the time of assay produced about twice as much urea as the old PICM-19 cultures that were 30 d post-passage at the time of assay. Although a meaningful statistical comparison could not be performed because of the limited number of observations, within age-of-culture group, there did not appear to be a difference in urea production between flight and ground-control cultures.

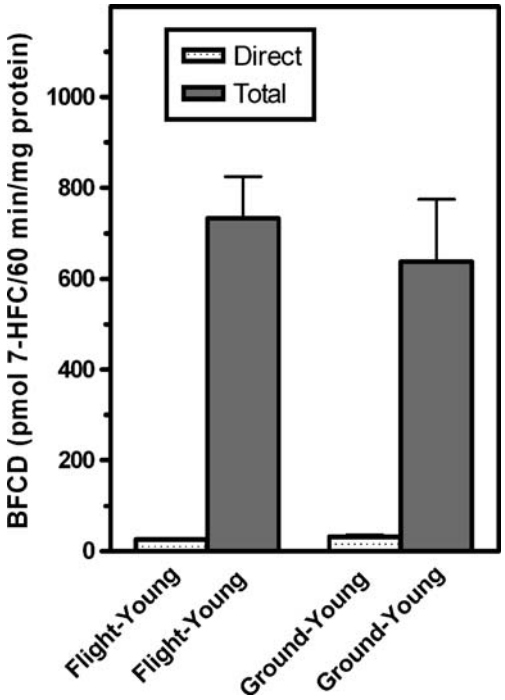


**Figure 5.** Induction of cytochrome P450 activity in 16-d flight and ground-control PICM-19 cultures by rifampicin (Rif). Cultures were exposed to 50 μM Rif in complete medium for 24 h after which the induction medium was replaced with specific enzyme substrate buffer to detect BFCD activity as described in Materials and Methods. Young culture samples ($n$=3), i.e., 4-d-old cultures at the time of shuttle launch, were used for the analysis, and values are means±SEM of three independent experiments. Direct P450 activity is without treatment of samples with β-glucuronidase/arylsulfatase (see Materials and Methods). An STO–feeder-cell-only control was not available for assay in the experiment, but STO feeder cells have previously shown no cytochrome P450 activity, either with or without 3MC or Rif induction (Talbot et al. 1996, manuscript submitted). Data were analyzed by $t$ test; no significant difference observed.

*Gene Expression Levels in PICM-19 Cells Exposed to Microgravity.* The relative abundance of mRNA for several genes was assayed by quantitative real-time RT-PCR in flight and ground-control cell culture samples, both young and old. The genes chosen for analysis are listed in Table 1, and they included markers of hepatocyte function [AFP, ALB, TTR, and cytokeratins (KRT18, KRT8; Germain et al. 1988)], hepatocyte-enriched functional genes [HMOX1, hepatocyte growth factor receptor (MET)], and transcription factors known to be of importance for hepatocyte differentiation [NFKB, HNF1A, HNF4A (Rodríguez-Antona et al. 2002)]. None of the pig-specific primers amplified a product in the STO cells alone whereas, the β-actin primer common to both mouse and pig amplified a product with a comparable cycle threshold value for STO only cells and STO plus PICM-19 cells (data not shown). Furthermore, the expected $C_T$ shift to the right with the pig-specific β-actin primer was seen in all the PICM-19 flight and ground samples. The data show that for markers of differentiation and liver-related cell function there was little difference between flight and ground-control culture in either the young or old samples for most of the genes examined (Fig. 7). The only genes exhibiting a slight difference in the transcript between the two populations of PICM-19 cells were MET, HMOX1, and KRT8 whose level increased by 34%, 38%, and 38%, respectively, in the young flight cells and albumin, which decreased by 35% in the flight cells. A comparison between young and old PICM-19 cultures independent of flight revealed a consistent difference in the transcript level between three genes, MET, HNF1A, and SOD2. The three transcripts were consistently greater in the younger than older PICM-19 cells; 2FA vs 3FA and 2GA vs 3GA were 56% and 49%, respectively, for MET; 49% and 52% for HNF1A; and 63% and 50% for SOD2. The statistical significance of the data could not be assessed because of the limited number of independent observations (one sample for each category).

## Discussion

The results of the study had several outcomes. First, this was the first experiment flown in space involving a liver cell line and more specifically, a liver stem cell line. Second, the PICM-19 cells grew, differentiated, and functioned normally in the Opticell units, i.e., as they do in T-flask cultures, in both the flight and ground-control cultures. Third, the different ages of the cultures at launch did not have an appreciable effect on the outcomes. Fourth,

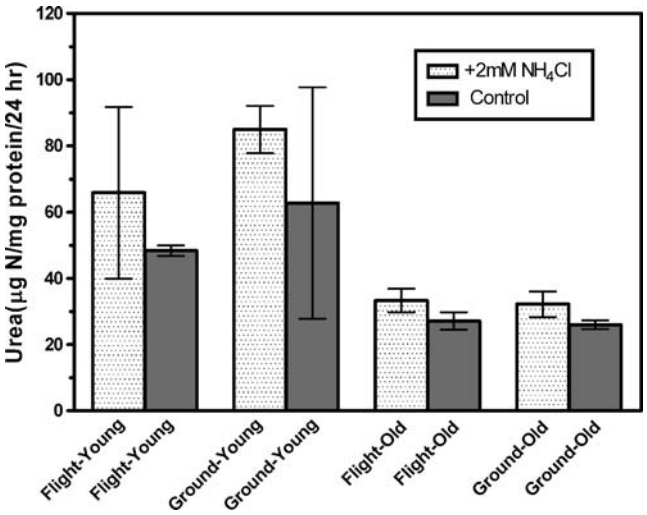


**Figure 6.** Urea production without (control) and with the addition of 2 mM of $NH_4Cl$ to the cell culture medium of flight and ground-control cultures. Note: $n$=2 samples per treatment, and *error bars* indicate individual values. In separate experiments, STO feeder cells alone do not produce urea (manuscript in preparation).

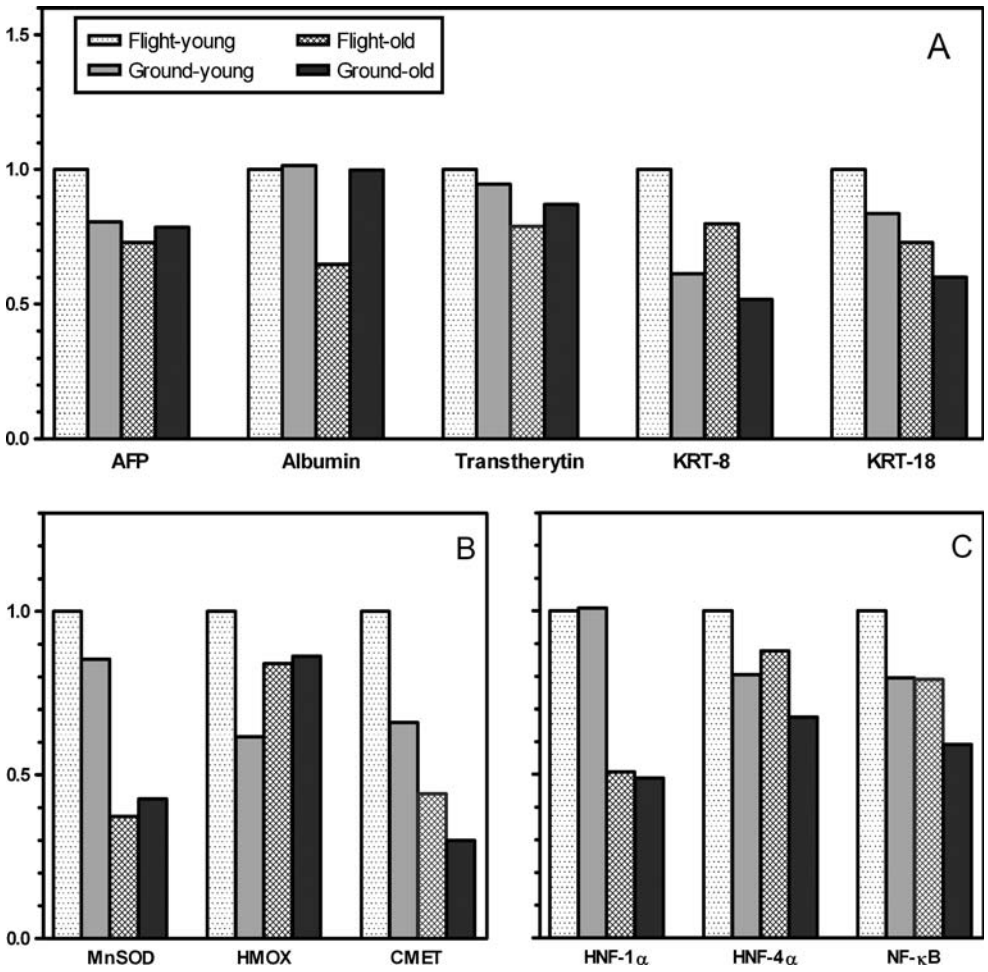


**Figure 7.** Quantitative RT-PCR gene expression analysis of *A*, hepatocyte marker genes, *B*, hepatocyte-enriched genes, and *C*, gene associated with hepatocyte and liver differentiation and development in PICM-19 flight and ground-control samples.

no new phenotypes were observed in the flight PICM-19 cell cultures, i.e., cells exhibiting dramatic differences from the usual PICM-19 character of growth or differentiation were not obvious. Fifth, and most importantly, from all observations and measures taken in the study, except for some minor changes in gene expression, there appeared to be no dramatic effects on the PICM-19 cultures that were exposed to the space environment for the 16 d of the STS-126 mission. However, because of the small number of independent culture samples, confidence in a lack of statistically significant differences between flight and ground samples in the biochemical assays or an apparent difference found in the gene expression assays should be tempered. That said, the very similar appearance between the flight and ground cultures by light and electron microscopy is remarkable. The results, therefore, are preliminary and should be viewed as qualitative in nature on the whole.

The flight PICM-19 cells (and ground-controls) displayed the typical morphology of pig fetal hepatocytes grown on an STO feeder layer when viewed by phase-contrast microscopy (Talbot et al. 1994a, 1994b). The ultrastructural feature perhaps most defining of hepatocytes, the specialized cell-to-cell unions that form biliary canaliculi were frequently observed in the flight PICM-19 cells by light and electron microscopy (Wanson et al. 1977; Talbot et al. 1996). The biliary canaliculi formed by the flight PICM-19 cells were similar to those found in vivo in thin sections of human embryonic, piglet, and rodent liver (Enzan et al. 1974; Wanson et al. 1977; Singh and Shahidi 1987), and, as with the ground-control PICM-19 cells, were responsive to added glucagon, i.e., displayed transcellular movement of fluid into the canaliculus (Macchiarelli and Motta 1993; Talbot et al. 2002).

Flight PICM-19 cells also produced urea and produced more urea in response to added ammonia, although there was not an apparent difference in comparison to the ground-control culture samples. In terms of absolute amounts of urea produced, the young flight and ground PICM-19 cultures that were 20 d post-passage at the time of assay produced about twice as much urea as the old PICM-19 cultures that were 30 d post-passage at the time of assay. An explanation for this difference is not immediately obvious, although past ground-based T-flask assays have shown that peak of metabolic performance falls off in PICM-19 cultures that are more than 4 wk old (unpublished

observations). Urea production in response to the addition of 2 mM ammonia was increased and would suggest that the metabolic machinery for urea production from amino acids and ammonia was maintained after exposure to microgravity. There was a very wide difference between duplicates in young that we cannot explain since the data is calculated based on a milligram cell protein basis which should have negated differences based on potential inconsistencies in cell numbers per sample tested.

The cytochrome P450 activities investigated (EROD and BFCD) were found to be similar between the ground-based and flight samples. These activities are similar to our observations in optimized cultures in T-25 flasks (on earth) and indicated that the Opticell environment was conducive to the maintenance of differentiated hepatocyte functions. The old cultures had less phase II activity when compared with younger cultures, a phenomenon that has not been previously investigated, but which may have resulted from the cultures being more than 4 wk of age, as speculated above for ureagenesis activity. The lack of fresh medium exchange during the experiment's culture period (necessitated by flight experimental design restraints) might have also contributed to such an effect, since the old cultures had a greater number of cells per unit area than the young cultures at the start of the experiment, and therefore, energy and metabolic substrates were probably lower in the old cultures towards the end, and this may have a negative impact on the older cells' metabolisms.

The gene expression data showed that, for some of the markers assayed, there were some differences found between flight and ground-control samples. Any differences were relatively minor and without the inclusion of additional independent samples, it could not be determined if the differences could reach statistical significance, however, none approached even a 2-fold difference. Thus, the assay mainly shows that the transcripts of factors regulating liver cell function, differentiation, and development were present in the in the PICM-19 cultures. Like the biochemical function assay, though, there was a consistent difference noted by age of culture for the transcript level between the three genes, MET, HNF1A, and SOD2. That is, the young PICM-19 cells, whether exposed to microgravity or not, had higher levels of these three transcripts than the old PICM-19 cells. Again, as speculated above, this might reflect a functional degradation in the older cells from an onset of senescent changes or from certain medium nutrients beginning to become limiting after 16 d without the addition of fresh culture medium.

Previously, other cell culture experiments in space, using either isolated cells or cell lines, have shown definite differences between the flight and ground-control cultures (Unsworth and Lelkes 1998; Freed and Vunjak-Novakovic 2002). Besides the delay involved in retrieving the STS-126 PICM-19 cultures from Edwards Air Force Base (17-h delay), what other possibilities might explain why there were so few differences found between flight and ground-control PICM-19 cultures? At least, a few other possibilities can be considered. Primary among these, and as already mentioned, is that not enough independent samples may have been available in the experiment to detect differences between flight and ground. Also, perhaps other types of experimental assays would show differences, e.g., global analysis of gene-expression rather than a candidate gene approach or assaying other metabolic functions besides urea production or phase I and II xenobiotic biotransformation. In many instances, past cell culture experiments in space, or in simulated microgravity on earth, have taken cells from their usual 2-dimensional monolayer culture format on plasticware and grown them 3-dimensionally as spheroids, unsupported or on microbeads or "scaffolding" of various kinds, so that the cells are free-floating in a low-shear environment. This leads to the adoption by the cells of more in vivo-like intracellular and intercellular features and up-regulation of cellular functions more typical of the in vivo tissue from which they were derived (Unsworth and Lelkes 1998). However, in the case of PICM-19 monolayer cultures, unlike the monolayer cultures of other cell lines, the PICM-19 cultures are really 3-dimensional in nature because the PICM-19 cells exist in a sandwich configuration between monolayers of STO feeder cells which arrange themselves above and below the PICM-19 cells (Talbot et al. 1994a, 1996, 2002). The PICM-19 monolayer cultures in the Opticell units, flight and ground-control, adopted the same configuration (as shown, Fig. 3*A*). Thus, PICM-19 cultures already starting out in a 3-dimensional growth and differentiation environment probably have less to gain in terms of acquisition of more in vivo-like characteristics than other monolayer-based cell cultures or cell lines that were subjected to space flight or simulated microgravity 3-dimensional culture conditions (Chang and Hughes-Fulford 2009). However, in other studies where adherent cells were grown in a standard monolayer format (e.g., on glass coverslips), or in cultures of anchorage-independent cells such as lymphocytes, observable and measurable effects of microgravity have been found (Morrison et al. 1992; Hughes-Fulford and Lewis 1996; Unsworth and Lelkes 1998; Freed and Vunjak-Novakovic 2002; Hatton et al. 2002; Kacena et al. 2003). So, a possibility may be that the STO feeder-cell-mediated 3-dimensional growth effects on the PICM-19 cells might have overshadowed the gravitational effects and that, if the PICM-19 cells were grown without feeder cells, giving the culture a 2-dimensional aspect, substantial differences might arise as microgravity might then induce 3-dimensional functionality in the PICM-19 cells, as observed

in previous 2-dimesional cell culture experiments in space (Hughes-Fulford and Lewis 1996).

In conclusion, the nature of the PICM-19 cells was not obviously changed by exposure to the space environment. However, the study's results should be viewed as preliminary since a greater number of observations are needed so that more meaningful statistical analyses can be performed. Also, different types of cell culture platforms than the one used in this study, e.g., 3-dimensional spheroid culture vs 2-dimensional culture, might be tested as has been done with other anchorage-dependent cell types, both in space and in simulated microgravity studies (Morrison et al. 1992; Unsworth and Lelkes 1998; Khaoustov et al. 2001; Freed and Vunjak-Novakovic 2002). Since the PICM-19 cell line is an effective in vitro model of not only hepatocyte and cholangiocyte function, but also of these cell types' growth and differentiation, the findings support the idea that, should astronauts suffer acute liver damage while in space, their livers would regenerate and repair normally in the microgravity environment. Finally, in neither the immediately assayed PICM-19 cells nor the PICM-19 cells continuously culture post-flight did there appear to be any new unique cellular characteristics, permanent or transient, that would enhance their utility for biotechnological purposes, such as their use in an extracorporeal bioartificial liver device.

**Acknowledgments** We thank Drs. Wesley Garrett and Julie Long for reading the manuscript and offering helpful editorial and scientific comments in its final preparation. We thank Amy Shannon, Ryan Willard, and John Meekin for their assistance in the laboratory and Ms. Jennifer Devich at KSC for logistical assistance. We thank the staff members of BioServe Space Technologies, University of Colorado, Boulder, CO, for their attention to detail and expertise in guiding the project to a successful conclusion, and especially thank Ms. Stefanie Countryman for her assistance, in general, and most especially for retrieving the samples from Edwards Air Force Base, CA. We also thank Scott McFarland of Boeing Aerospace and John Wayne Kennedy for guidance, meeting support, and encouragement in the project.

This work was supported by NASA, BioServe Space Technologies, Inc., Zero Gravity, Inc., Hepalife Technologies, Inc., and the State of Maryland (TEDCO). Mention of trade names or commercial products in this publication is solely for the purpose of providing specific information and does not imply recommendation or endorsement by the US Department of Agriculture.

## References

Abraham S.; Klein H. P.; Lin C. Y.; Volkmann C. The effects of space flight on some rat liver enzymes regulating carbohydrate and lipid metabolism. *Adv Space Res* 1: 199–217; 1981.

Abraham S.; Lin C. Y.; Volkmann C. M.; Klein H. P. Biochemical changes in rat liver after 18.5 d of spaceflight. *Proc Soc Exp Biol Med* 172: 334–9; 1983.

Ahlers I.; Tigranyan R. A.; Praslicka M. The effect of artificial gravity on plasma and tissue lipids in rats: the Cosmos 936 experiment. *Adv Space Res* 1: 193–8; 1981.

Blomberg L. A.; Long E. L.; Sonstegard T. S.; Van Tassell C. P.; Dobrinsky J. R.; Zuelke K. A. Serial analysis of gene expression during elongation of the peri-implantation porcine trophectoderm (conceptus). *Physiol Genomics* 20: 188–94; 2005.

Brooks F. A.; Gardner R. L. The origin and efficient derivation of embryonic stem cells in the mouse. *Proc Natl Acad Sci USA* 94: 5709–5712; 1997.

Chang T. T.; Hughes-Fulford M. Monolayer and spheroid culture of human liver hepatocellular carcinoma cell line cells demonstrate distinct global gene expression patterns and functional phenotypes. *Tissue Eng Part A* 15: 559–67; 2009.

Clavin M.; Gazenko O. G. (eds). Foundations of space biology and medicine, NASA SP-374. National Aeronautics and Space Administration Scientific and Technical Information Office, Washington, DC; 1975.

Clément G. Fundamentals of space medicine. Springer, Dordrecht, The Netherlands; 2005.

Clement J. Q.; Lacy S. M.; Wilson B. L. Genome-wide gene expression profiling of microgravity effect on human liver cells. *J Gravit Physiol* 14: P121–2; 2007.

Denisova L. A.; Lavrova E. A.; Natochin Iu V; Serova L. V. Water and electrolyte content of the organs and tissues of male rats following a flight on the Kosmos 1667 biosatellite. *Kosm Biol Aviakosm Med* 22: 33–7; 1988.

Donato M. T.; Gomez-Lechon M. J.; Castell J. V. A microassay for measuring sytochrome P450IA1 and P450IIB1 activities in intact human and rat hepatocytes cultured on 96-well plates. *Anal Biochem* 213: 29–33; 1993.

Enzan H.; Ohkita T.; Fujuta H.; Iijima S. Light and electron microscopic studies on the development of periportal bile ducts of the human embryo. *Acta Pathol Jpn* 24: 427–447; 1974.

Freed L. E.; Vunjak-Novakovic G. Spaceflight bioreactor studies of cells and tissues. *Adv Space Biol Med* 8: 177–95; 2002.

Germain L.; Blouin M. J.; Marceau N. Biliary epithelial and hepatocytic cell lineage relationships in embryonic rat liver as determined by the differential expression of cytokeratins, alpha-fetoprotein, albumin, and cell surface-exposed components. *Cancer Res* 48: 4909–4918; 1988.

Gilloteaux J.; Karkare S.; Kelly T.; Hawkins W. S. Ultrastructural aspects of human gallbladder epithelial cells in cholelithiasis: production of anionic mucus. *Microsc Res Tech* 38: 643–659; 1997.

Guyton A. C.; Hall J. E. Textbook of medical physiology. 11th ed. Elsevier Saunders, Philadelphia; 2006.

Hatton J. P.; Gaubert F.; Cazenave J. P.; Schmitt D. Microgravity modifies protein kinase C isoform translocation in the human monocytic cell line U937 and human peripheral blood T-cells. *J Cell Biochem* 87: 39–50; 2002.

Hughes-Fulford M.; Lewis M. L. Effects of microgravity on osteoblast growth activation. *Exp Cell Res* 224: 103–9; 1996.

Husson A.; Buquet C.; Vaillant R. Induction of the five urea-cycle enzymes by glucagon in cultured foetal rat hepatocytes. *Differentiation* 35: 212–8; 1987.

Ikuzawa M.; Asashima M. Global expression of simulated microgravity-responsive genes in Xenopus liver cells. *Zoolog Sci* 25: 828–37; 2008.

Ishii M.; Vroman B.; LaRusso N. F. Isolation and morphologic characterization of bile duct epithelial cells from normal rat liver. *Gastroenterology* 97: 1236–1247; 1989.

Kacena M. A.; Todd P.; Landis W. J. Osteoblasts subjected to spaceflight and simulated space shuttle launch conditions. *In Vitro Cell Dev Biol Anim* 39: 454–9; 2003.

Khaoustov V. I.; Darlington G. J.; Soriano H. E.; Krishnan B.; Risin D.; Pellis N. R.; Yoffe B. Induction of three-dimensional assembly of human liver cells by simulated microgravity. *In Vitro Cell Dev Biol Anim* 35: 501–9; 1999.

Khaoustov V. I.; Risin D.; Pellis N. R.; Yoffe B. Microarray analysis of genes differentially expressed in HepG2 cells cultured in simulated microgravity: preliminary report. *In Vitro Cell Dev Biol Anim* 37: 84–8; 2001.

Komolova G. S.; Zakaznov A. V.; Makeeva V. F. Effect of weightlessness on the DNA replicative function of rat hepatocytes. *Kosm Biol Aviakosm Med* 21: 31–4; 1987.

Macchiarelli G.; Motta P. M. Ultrastructure of the hepatocyte. In: Tavoloni N.; Berk P. D. (eds) Hepatic transport and bile secretion: physiology and pathophysiology. Raven Press, New York, pp 103–116; 1993.

Macho L.; Fickova M.; Nemeth S.; Svabova E.; Serova L.; Popova I. The effect of space flight on the board of the satellite Cosmos 2044 on plasma hormone levels and liver enzyme activities of rats. *Acta Astronaut* 24: 329–32; 1991a.

Macho L.; Ficková M.; Zórad S.; Serova L.; Popova I. Plasma insulin levels and insulin receptors in liver and adipose tissue of rats after space flight. *Physiologist* 34(1 Suppl): S90–1; 1991b.

Macho L.; Nemeth S.; Kvetnansky R.; Fickova M.; Tigranian R. A.; Serova L. Metabolic changes in the animals subjected to space flight. *Acta Astronaut* 9: 385–9; 1982.

Merrill Jr. A. H.; Hoel M.; Wang E.; Mullins R. E.; Hargrove J. L.; Jones D. P.; Popova I. A. Altered carbohydrate, lipid, and xenobiotic metabolism by liver from rats flown on Cosmos 1887. *FASEB J* 1: 95–100; 1990.

Merrill Jr. A. H.; Wang E.; Jones D. P.; Hargrove J. L. Hepatic function in rats after spaceflight: effects on lipids, glycogen, and enzymes. *Am J Physiol* 252(2 Pt 2): R222–6; 1987.

Metoki K.; Hommes F. A. A possible rate limiting factor in urea synthesis by isolated hepatocytes: the transport of ornithine into hepatocytes and mitochondria. *Int J Biochem* 16: 1155–7; 1984.

Misurova E.; Tigranyan R. A.; Praslicka M. Changes of deoxyribonucleoprotein in the spleen, thymus and liver of rats exposed to weightlessness and artificial gravity aboard the Cosmos biosatellites. *Adv Space Res* 1: 225–30; 1981.

Miyake M.; Yamasaki M.; Katahira K.; Waki H.; Katsuda S.; Ijiri K.; Shimizu T. Effects of the spaceflight on organ-development in the neonatal rats: results in the Neurolab (STS-90). *Biol Sci Space* 16: 209–10; 2002.

Morrison D. R.; Chapes S. K.; Guikema J. A.; Spooner B. S.; Lewis M. L. Experiments with suspended cells on the Space Shuttle. *Physiologist* 35(1 Suppl): S31–4; 1992.

Nemeth S.; Macho L.; Palkovic M.; Skottova N.; Tigranyan R. A. Metabolic changes in rats subjected to space flight for 18.5 d in the biosatellite Cosmos 936. *Adv Space Res* 1: 219–24; 1981.

Nemeth S.; Tigranian R. A. Activity of various liver enzymes in rats following a flight aboard the Cosmos-936 biosatellite. *Kosm Biol Aviakosm Med.* 16: 77–80; 1982.

Popova I. A.; Zabolotskaia I. V.; Kurkina L. M. The effects of space flights on the lipid composition of blood, adrenal glands and liver in rats. *Aviakosm Ekolog Med* 33: 47–51; 1999.

Rabot S.; Szylit O.; Nugon-Baudon L.; Meslin J. C.; Vaissade P.; Popot F.; Viso M. Variations in digestive physiology of rats after short duration flights aboard the US space shuttle. *Dig Dis Sci* 45: 1687–95; 2000.

Racine R. N.; Cormier S. M. Effect of spaceflight on rat hepatocytes: a morphometric study. *J Appl Physiol* 73(2 Suppl): 136S–141S; 1992.

Rodríguez-Antona C.; Donato M. T.; Boobis A.; Edwards R. J.; Watts P. S.; Castell J. V.; Gómez-Lechón M. J. Cytochrome P450 expression in human hepatocytes and hepatoma cell lines: molecular mechanisms that determine lower expression in cultured cells. *Xenobiotica* 32: 505–20; 2002.

Sen S.; Williams R. New liver support devices in acute liver failure: a critical evaluation. *Semin Liver Dis* 23(3): 283–294; 2003.

Singh A.; Shahidi E. Ultrastructure of piglet liver. In: Tumbleson M. E. (ed) Swine in biomedical research, Vol. 1. Plenum Press, New York, p 84; 1987.

Strain A. J.; Neuberger J. M. A bioartificial liver—state of the art. *Science* 295: 1005–1009; 2002.

Sussman N. L.; Kelly J. H. The artifical liver. *Sci Am* 2: 68–77; 1995.

Talbot N. C.; Caperna T. J. Selective and organotypic culture of intrahepatic bile duct cells from adult pig liver. *In Vitro Cell Dev Biol* 34A: 785–798; 1998.

Talbot N. C.; Paape M. J. Continuous culture of pig tissue-derived macrophages. *Meth Cell Sci* 18: 315–327; 1996.

Talbot N. C.; Caperna T. J.; Lebow L. T.; Moscioni D.; Pursel V. G.; Rexroad Jr. C. E. Ultrastructure, enzymatic, and transport properties of the PICM-19 bipotent liver cell line. *Exp Cell Res* 225: 22–34; 1996.

Talbot N. C.; Caperna T. J.; Wells K. D. The PICM-19 cell line as an in vitro model of liver bile ductules: effects of cAMP inducers, biopeptides and pH. *Cells Tissues Organs* 171: 99–116; 2002.

Talbot N. C.; Powell A.; Garrett W.; Edwards J. L.; Rexroad Jr. C. E. Ultrastructural and karyotypic examination of in vitro produced bovine embryos developed in the sheep uterus. *Tissue Cell* 32: 9–27; 2000.

Talbot N. C.; Pursel V. G.; Rexroad Jr. C. E.; Caperna T. J.; Powell A. M.; Stone R. T. Colony isolation and secondary culture of fetal porcine hepatocytes on STO feeder cells. *In Vitro Cell Dev Biol* 30A: 851–858; 1994a.

Talbot N. C.; Rexroad Jr. C. E.; Powell A.; Pursel V. G.; Caperna T. J.; Ogg S. L.; Nel N. D. A continuous culture of pluripotent fetal hepatocytes derived from the 8-day epiblast of the pig. *In Vitro Cell Dev Biol* 30A: 843–850; 1994b.

Talbot N. C.; Jr C. E.; Rexroad V. G. Pursel; Powell A. M.; Nel N. D. Culturing the epiblast cells of the pig blastocyst. *In Vitro Cell Dev Biol* 29A: 543–554; 1993.

Tanaka M. A histochemical study on the activity of gamma-glytamyl transpeptidase in liver disease. *Acta Path Jpn* 24: 651–665; 1974.

Tietze K. J.; Putcha L. Factors affecting drug bioavailability in space. *J Clin Pharmacol* 34: 671–6; 1994.

Triebwasser K. C.; Freedland R. A. The effect of glucagon on ureagenesis from ammonia by isolated rat hepatocytes. *Biochem Biophys Res Commun* 76: 1159–65; 1977.

Unsworth B. R.; Lelkes P. I. Growing tissues in microgravity. *Nat Med* 4: 901–7; 1998.

Wanson J. C.; Drochmans P.; Mosselmans R.; Ronveaux M. F. Adult rat hepatocytes in primary monolayer culture: ultra-structural characteristics of intercellular contacts and cell membrane differentiations. *J Cell Biol* 74: 858–877; 1977.

Wybenga D. R.; Di Giorgio J.; Pileggi V. J. Manual and automated methods for urea nitrogen measurement in whole serum. *Clin Chem* 17: 891–5; 1971.

Yamashita M.; Izumi-Kurotani A.; Imamizo M.; Koike H.; Okuno M.; Pfeiffer C. J.; Komazaki S.; Sasaki F.; Ohira Y.; Kashima I.; Kikuyama S.; Ohnishi T.; Mogami Y.; Asashima M. Japanese red-bellied newts in space—AstroNewt experiment on space shuttle IML-2 and space flyer unit. *Biol Sci Space* 15: 96–s103; 2001.